Soft Matter

RSC Publishing

PAPER

View Article Online
View Journal | View Issue

Cite this: *Soft Matter*, 2013, **9**, 9579

Non-linear surface dilatational rheology as a tool for understanding microstructures of air/water interfaces stabilized by oligofructose fatty acid esters

Silvia E. H. J. van Kempen,[ab] Henk A. Schols,[c] Erik van der Linden[a] and Leonard M. C. Sagis*[a]

In this paper, the rheological response of air/water interfaces, stabilized by various oligofructose fatty acid esters, to oscillatory dilatational deformations was studied and compared to the response of interfaces stabilized by sucrose esters. We have followed a traditional approach to surface rheology, where the development of the modulus as a function of time is studied as well as the frequency dependence of the modulus. We also adopted a different approach where we investigate in detail the amplitude dependence of the modulus. Finally, we studied the temperature dependence. We show that for an accurate characterization of the dilatational rheology of fluid–fluid interfaces with a complex microstructure, a protocol should be used that not only involves variations of surface pressure, frequency, and temperature, but also establishes amplitude dependence. We show that Lissajous plots of surface pressure *versus* deformation can be useful tools to help interpret surface dilatational behavior in terms of interfacial microstructure. The rheological response of interfaces stabilized by oligofructose esters differed significantly from the response of those stabilized by sucrose esters. Sucrose esters behaved like typical low molecular weight surfactants, and gave interfaces with relatively low moduli, a frequency scaling of the dilatational modulus with an exponent close to 0.5, and displayed no asymmetries in Lissajous plots. In contrast, the oligofructose esters gave, depending on the fatty acid tail, relatively high moduli, almost independent of frequency. Significant asymmetries were observed in the Lissajous plots, with strain hardening during compression and strain softening during extension. Our results suggest that the unusual rheological properties of interfaces stabilized by oligofructose esters may be the result of the formation of a two-dimensional soft glass phase by the oligofructose part of the ester.

Received 27th June 2013
Accepted 8th August 2013

DOI: 10.1039/c3sm51770e

www.rsc.org/softmatter

1 Introduction

Many food products or parts of food products consist of foams,[1] such as the head of beer, whipped cream, mousses, cappuccino foam, and bread.[2] To improve the stability of foams, surface active molecules are added to foam formulations. These molecules adsorb at the air/water interface where they significantly alter the interfacial properties. Although the relation between interfacial properties and macroscopic properties such as foam stabilizing capabilities is still an active area of research, most researchers agree that the study of interfacial rheology is relevant with respect to foaming properties.[3–5]

For low molecular weight (LMW) surfactants, the dilatational rheological response of the interface at low surface concentrations will be mostly influenced by transport of monomers from the bulk to the interface.[5] Above the critical micelle concentration, the presence of micelles in the subphase complicates matters, since now, in addition to the transport of monomers to and from the interface, one has to take into account the transition from micelles to monomers.[6] With increasing surface concentration of the surfactant, it becomes more likely that a high modulus is caused by structure formation at the interface. As already demonstrated by Rodríguez Patino *et al.*,[7,8] some surfactants can exhibit rich phase behavior with moduli that are strongly dependent on the degree of surface coverage and the microstructure of the surface layer.

The dilatational rheological response of an interface will depend on the ratio of the characteristic time scale that is related to the transport of molecules from the bulk to the interface and the characteristic time scale that is related to the rate of interfacial deformation. Therefore, frequency sweeps are often used to characterize the rheological response of interfacial layers in more detail. The slope in a double logarithmic plot of modulus *versus* frequency can provide useful information about the interfacial kinetics. Two specific cases in the response are a

[a]*Laboratory of Physics and Physical Chemistry of Foods, Wageningen University, Bomenweg 2, 6703 HD Wageningen, The Netherlands. E-mail: leonard.sagis@wur.nl; Fax: +31 317 483669; Tel: +31 317 485023*

[b]*Dutch Polymer Institute DPI, P.O. Box 902, 5600 AX Eindhoven, The Netherlands*

[c]*Laboratory of Food Chemistry, Wageningen University, Bomenweg 2, 6703 HD Wageningen, The Netherlands*

slope of 0 and a slope of 0.5. A slope of 0 implies a completely elastic interface and is often found at very high frequencies, where the deformation is so fast that diffusion from the bulk to the interface is negligible. In contrast, a slope of 0.5 corresponds to processes that are completely diffusion controlled, as explained in the Lucassen van den Tempel model,[9] a value which is often found at very low frequencies.[10]

While frequency sweeps are often performed during the study of interfacial dilatational rheology of surfactant stabilized interfaces, amplitude sweeps are much less common. Most authors do not investigate any possible dependence of rheological properties on the magnitude of the deformation, and simply assume that they are measuring within the linear viscoelastic regime, without providing the experimental data to support their assumption.[11] These amplitude sweeps are considered standard practice in bulk rheology to establish whether experiments are performed in the linear viscoelastic regime. When the dilatational modulus is a result of structure formation at the interface, the interfacial microstructure may be affected by the applied deformation, and we would expect a dependence of the rheological properties on amplitude. To address this issue, in this paper we performed a detailed analysis of the amplitude dependence of the surface dilatational modulus.

Oligofructose fatty acid esters have been described recently as molecules that provide air/water interfaces with relatively high surface dilatational moduli, and that have excellent foam stabilizing capabilities.[12–14] They are surface active components that can be synthesized with a wide range of amphiphilicity and thus functionality. This wide range is accomplished by changing the fatty acid chain length and the degree of esterification. The oligofructose used was a mixture of oligomers with a degree of polymerization varying between 2 and 8 (average 4.4). Consequently, the resulting esters are also mixtures. In a previous paper, we have reported the equilibrium surface tension and surface dilatational modulus of air/water interfaces stabilized by oligofructose fatty acid mono-esters with different fatty acid chain lengths.[14] We have shown that interfaces stabilized by oligofructose esters containing longer fatty acid chains had a significantly higher dilatational modulus than those stabilized by esters containing shorter fatty acid chains. Furthermore, we observed that these high dilatational moduli were accompanied by extremely high standard deviations. We attributed these extremely high standard deviations to the fact that measurements may have been taken outside of the linear viscoelastic regime.

The purpose of this paper was to study the dilatational rheological properties of air/water interfaces stabilized by oligofructose fatty acid esters with variations in the fatty acid chain, as a function of the surface pressure, frequency, deformation amplitude, and temperature. To study the influence of the size of the hydrophilic group, also sucrose esters were studied. First, we adopted a traditional approach to surface rheology. In Section 3.1 we focus on the development of the modulus during time sweeps. We have also studied the surface rheological properties of the interfaces after reaching equilibrium. We performed frequency sweeps, which are discussed in Section 3.2. Next, we adopted a different approach, where we studied in detail the amplitude dependence of the modulus, which is discussed in Section 3.3. Finally, for some of the samples we have performed temperature sweeps, which are discussed in Section 3.4.

2 Materials and methods

2.1 Materials

Palmitoleic acid was obtained from Sigma Aldrich (Steinheim, Germany). Oligofructose fatty acid esters (Fig. 1A) were prepared according to a previously described protocol, by esterification of fatty acids with oligofructose with a degree of polymerization ranging from 2 to 8, using lipase as a catalyst. Four different fatty acid chain lengths were used (C8, C12, C16 and C18). The crude products contained mostly mono-esters, but also small amounts of di-esters. The products were fractionated to separate the fractions with different degrees of esterification. Using MALDI-TOF MS and NMR we established the purity (>90% for mono-esters, >80% for di-esters) of the purified fractions.[14] Additionally, an ester with palmitoleic acid (C16:1) as the hydrophobic group was produced using the procedure as previously described for palmitic acid esters.[14] Using MALDI-TOF MS[14] a purity of 100% was established.

Sucrose monolaurate (≥97%, Fig. 1B) was obtained from Sigma Aldrich (Steinheim, Germany). Sucrose esters with fatty acid chain lengths C16 and C18 (RYOTO esters S1670 and P1670) were obtained from Mitsubishi-Kagaku Foods Corporation (Tokyo, Japan). Both S1670 and P1670 are crude products. According to the manufacturer, S1670 consists of 75% mono-esters and 25% di-, tri-, and poly-esters. The fatty acids consist of 70% of stearic acid. P1670 consists of 80% mono-esters and 20% di-, tri-, and poly-esters. The fatty acids consist of 80% of palmitic acid. These products were used without further purification.

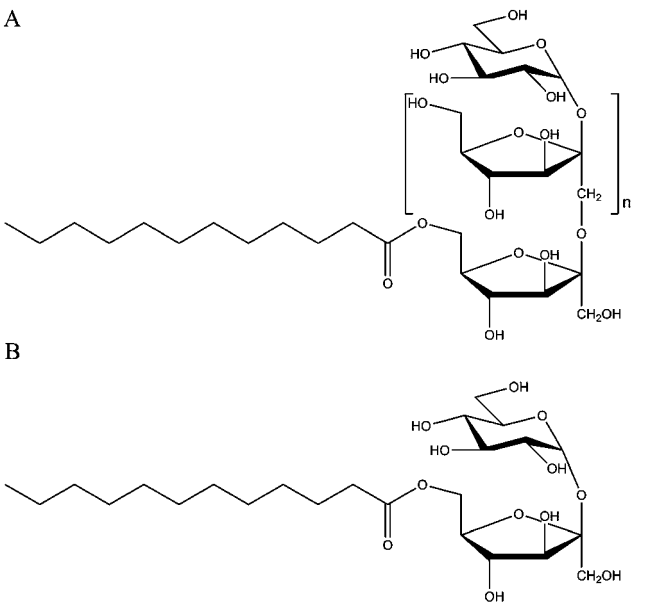

Fig. 1 Chemical structure of oligofructose fatty acid ester (A) and sucrose ester (B).

2.2 Methods

2.2.1 Sample preparation. Samples were prepared by dissolving the surfactant in Millipore water (Millipore corporation, Billerica, Massachusetts, USA). For esters with longer fatty acid chains (C16 and C18) mild heating (max. 70 °C) was applied to improve the dispersion of the esters in the liquid.

2.2.2 Determination of surface tension and surface dilatational modulus. The surface tension and complex surface dilatational modulus of the air/water interface were determined using a profile analysis tensiometer (Sinterface, Berlin, Germany). During time sweeps, sinusoidal oscillations with an amplitude of 5% and a frequency of 0.1 Hz were applied. From the intensity and phase of the first harmonic of the Fourier transform of the oscillating surface tension signal, the complex surface dilatational modulus was determined. The experiments consisted of 25 cycles of oscillations that were alternated with 1 cycle of rest. These experiments were continued until equilibrium was reached. The time sweeps were followed by a frequency sweep where the frequency was increased stepwise from 0.005 Hz to 1 Hz at an amplitude of 5%. The slope of a double logarithmic plot of complex surface dilatational modulus *versus* frequency was determined using linear regression. The quality of the linear regression fit was generally very high. At the highest frequencies, the fit used to establish the first-harmonic Fourier moduli was not always of sufficient quality, which reduced the accuracy of the values for the moduli. Therefore, these values were excluded from the regression fit. The experimental series was finished with an amplitude sweep, where the amplitude was increased stepwise from 1.5% to 30% at a frequency of 0.1 Hz. All experiments were performed at 25 °C.

For the temperature sweeps an automated drop tensiometer was used (ITCONCEPT, Longessaigne, France). The reported temperature is the temperature of the cuvette holder and may slightly differ from the actual sample temperature. Similar to the experiments performed with the profile analysis tensiometer, an amplitude of 5% and a frequency 0.1 Hz were used.

2.2.3 Analysis of amplitude sweeps. In a paper by Ewoldt *et al.*,[15] the authors demonstrated the limitations of using first-harmonic Fourier moduli, which are the common output of rheometers. The profile analysis tensiometer that was used in our study also reports first-harmonic Fourier moduli, and particularly for large deformations these dilatational moduli will have limited physical meaning.

For oscillatory shear experiments on bulk fluids Ewoldt *et al.*[15] have shown how the raw signal of a rheometer, expressed as a Lissajous plot of stress *versus* strain, may be analyzed to reveal the presence of intracycle strain thinning and thickening. They have defined a minimum strain shear modulus (G_M), a large strain shear modulus (G_L) and a strain-stiffening ratio S to quantify the degree of non-linearity:

$$S \equiv \frac{G_L - G_M}{G_L} \quad (1)$$

here $S = 0$ may be interpreted as a linear elastic response, $S > 0$ indicates intracycle strain stiffening, and $S < 0$ corresponds to intracycle strain softening.

In this paper we have extended this approach to analyze surface dilatational oscillatory experiments. We have used the output of the profile analysis tensiometer to construct Lissajous plots, of the surface pressure ($\Pi = \gamma - \gamma_0$) *versus* deformation ($\delta A/A_0$). Here $\delta A = A - A_0$, γ and A are the surface tension and area of the deformed interface, and γ_0 and A_0 are the surface tension and area of the non-deformed interface. An example of these plots is shown in Fig. 2.

In most cases, we found a different response in compression than in extension. Therefore, we defined the following factors in the analysis of the curves in this paper: $E_{L,E}$, defined as the large strain modulus in extension, $E_{M,E}$, defined as the minimum strain modulus in extension, $E_{L,C}$, defined as the large strain modulus in compression, and $E_{M,C}$, defined as the minimum strain modulus in compression. In Fig. 2 the method for determining these factors is demonstrated. Furthermore, we have defined two strain-stiffening ratios (S), S_{ext} and S_{com}:

$$S_{ext} \equiv \frac{E_{L,E} - E_{M,E}}{E_{L,E}} \quad (2)$$

$$S_{com} \equiv \frac{E_{L,C} - E_{M,C}}{E_{L,C}} \quad (3)$$

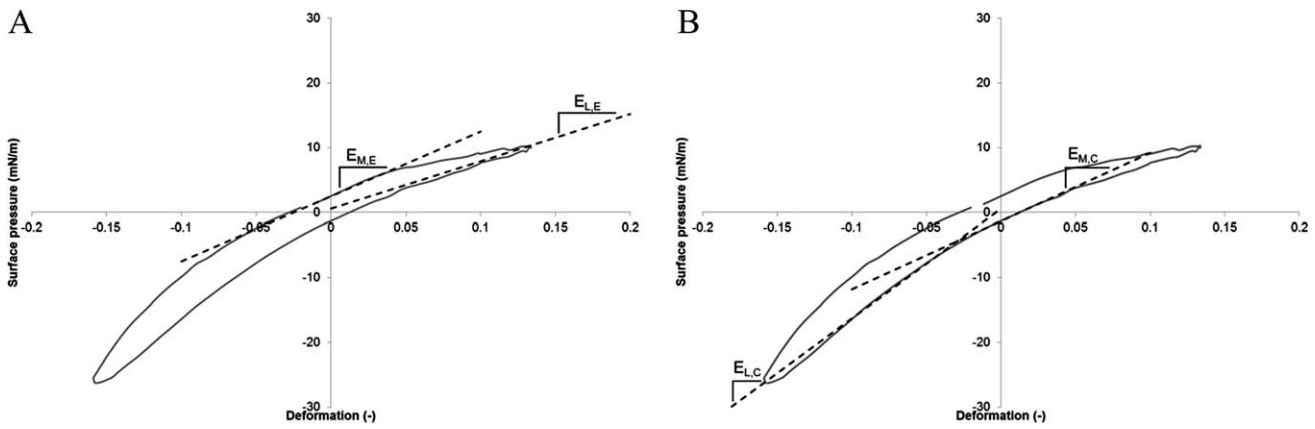

Fig. 2 Determination of the minimum strain modulus and the large strain modulus in extension (A) and compression (B).

with these factors, it is possible to quantify the degree of non-linearity and distinguish between the response in compression and extension. For both factors, $S = 0$ may be interpreted as a linear elastic response, $S > 0$ indicates intracycle strain stiffening, and $S < 0$ corresponds to intracycle strain softening.

In addition to the analysis described in this paper, the observed surface oscillation response could be expanded in a Fourier series[16,17] or a series of Chebyshev polynomials.[15] However, we believe that in this situation the graphical presentation leads to more insight.

3 Results & discussion

In this study, the dilatational rheological properties of air/water interfaces stabilized by oligofructose fatty acid esters were investigated. Due to the expected impact on functionality, we have studied the following variations in the molecular structure: length of the fatty acid chain, degree of esterification, degree of saturation of the fatty acid chain and size of the hydrophilic group. To study the influence of the length of the fatty acid chain, oligofructose mono-esters containing saturated fatty acids with chain lengths of 8, 12, 16 and 18 carbon atoms, designated OF-C8m, OF-C12m, OF-C16m and OF-C18m, were studied. To study the influence of the degree of esterification, in addition to mono-esters, also di-esters with fatty acid chain lengths 8 and 12, designated OF-C8d and OF-C12d, were investigated. To study the influence of the degree of saturation of the fatty acid chain, in addition to OF-C16m, an oligofructose ester with the mono-unsaturated fatty acid *cis*-9-hexadecenoic acid as the hydrophobic group, designated OF-C16:1m, was studied. To study the influence of the size of the hydrophilic group, sucrose esters were also investigated. These were a mono-ester with fatty acid chain length C12, designated S-C12m, and two crude samples composed of a mixture of mono-esters and di-esters with fatty acid chain lengths C16 and C18, designated S-C16 and S-C18. First, we follow a traditional approach where we treat the development of the complex surface dilatational modulus as a function of the surface pressure (Section 3.1) during time sweeps and the frequency dependence of the complex dilatational modulus of the interfaces after reaching equilibrium (Section 3.2). Next, we adopt a different approach and present a detailed study of the dependence of the complex moduli on the amplitude (Section 3.3). Also, we focus on the temperature dependence (Section 3.4) of the complex moduli.

3.1 Traditional approach to surface rheology: development of the modulus during time sweeps

To establish the dependence of the complex surface dilatational modulus on surface pressure, a series of time sweeps was performed using samples with a wide range of bulk concentrations of the ester, to cover a wide range of surface pressures. In Fig. 3 the results of these experiments are shown for the oligofructose (saturated) mono-esters and di-esters. In a previous paper[18] we have measured surface tension as a function of bulk concentration of these esters, and reported their critical micelle concentration (CMC). The surface pressure at these CMC values (π_{CMC}) differed slightly as a function of the molecular structure of the ester, and is indicated in Fig. 3.

For all samples, a sharp increase in the surface dilatational modulus is observed at very low surface pressures (0–3 mN m^{-1}). In some cases there is a high degree of variability in the values for the surface dilatational modulus at similar surface pressures. It seems, however, that after the initial increase in the surface dilatational modulus, a (semi)plateau value is reached over a wide range of surface pressures. The plateau value of the surface dilatational modulus is dependent on the molecular structure: with increasing fatty acid chain length or degree of esterification, the plateau value increases. For example, the plateau value obtained for OF-C12m (Fig. 3C) was around 20 mN m^{-1}, while for OF-C18m (Fig. 3F) it was around 60 mN m^{-1}. At surface pressures lower than π_{CMC}, there are no micelles present in the bulk. This means that during compression and extension, only single molecules will exchange between bulk and interface. Since an increasing fatty acid chain length or degree of esterification will increase the hydrophobicity of the molecule, the affinity of these molecules for the interface will also increase. This means that exchange between bulk and interface is less likely to occur, leading to a higher value for the dilatational modulus.

With increasing surface pressure, the degree of surface coverage is increased. This means that interactions between the molecules become more and more important. When the degree of surface coverage is sufficiently high, and there are sufficiently strong interactions between the molecules, it is possible that interfacial mesophases are formed. We hypothesize that this could be a glass phase formed by the oligofructose part of the esters or a crystalline phase formed by the fatty acid chains. The dilatational modulus is then no longer exclusively determined by exchange of the esters with the subphase, but also by in-plane interactions (deviatoric stresses and/or bending stresses).

The influence of the degree of saturation of the fatty acid chain on the rheological response was investigated by studying the complex surface dilatational modulus as a function of the surface pressure for OF-C16:1m (Fig. 4). The shape of the curve is similar to the curves in Fig. 3. Also here a plateau value for the surface dilatational modulus was obtained. The plateau value of the surface dilatational modulus obtained for OF-C16:1m was comparable to the one obtained for OF-C16m.

The curves in Fig. 3 and 4 also present some curious features that are more difficult to explain. As already mentioned, in some cases there is a high degree of variation in the surface dilatational modulus at similar surface pressures. This degree of variation is quite pronounced in the intermediate surface pressure regime of OF-C8m (Fig. 3A) and the high surface pressure regime of OF-C16m (Fig. 3E). A possible explanation for the variations may be that the deformation amplitude used in these experiments was above the maximum linear strain, and therefore the measurements were not in the linear response regime. We will say more about this issue in Section 3.3.

Furthermore, in some cases the surface dilatational modulus starts to deviate from the plateau value at surface pressures

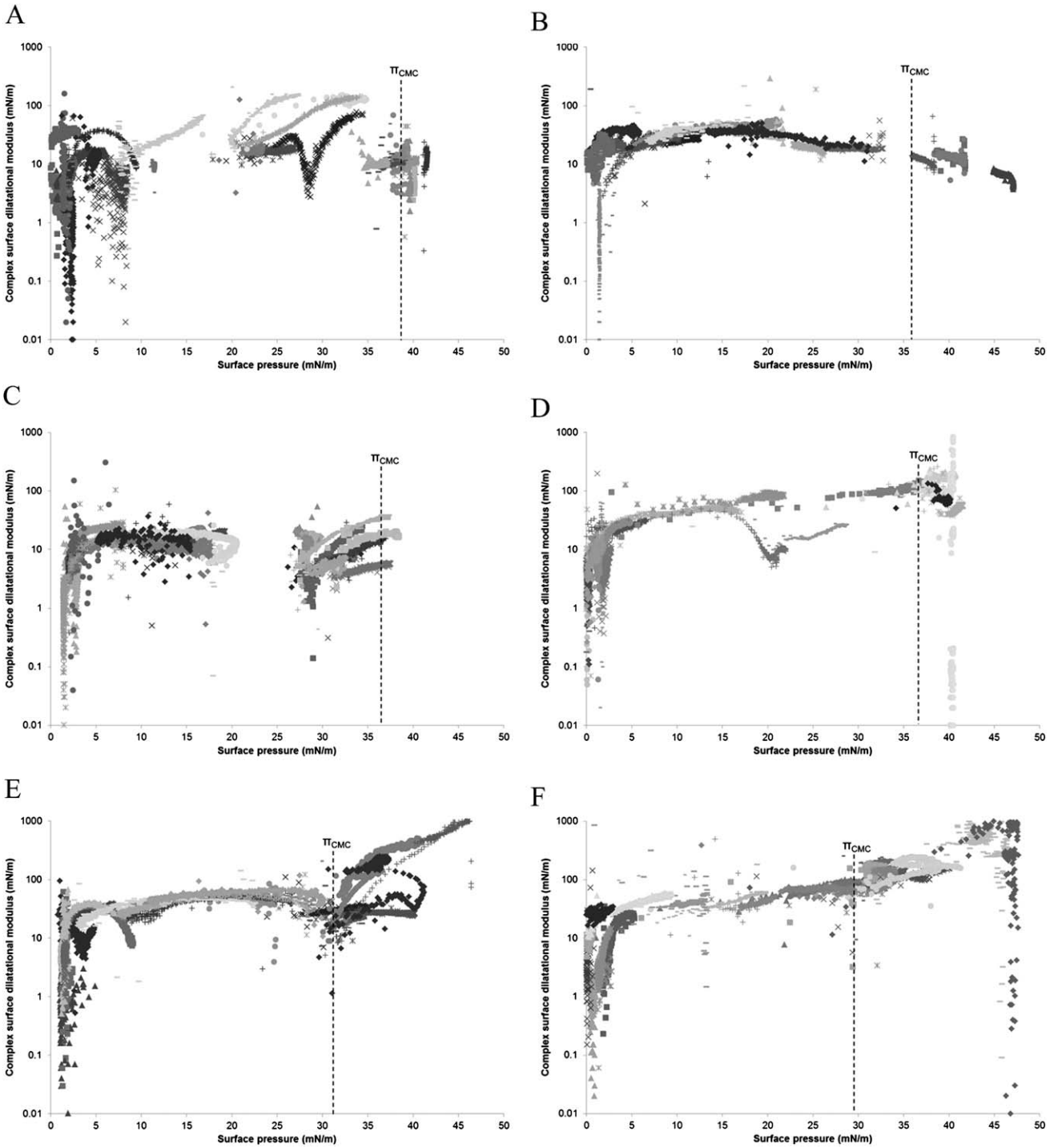

Fig. 3 Complex surface dilatational modulus as a function of surface pressure of air/water interfaces stabilized by oligofructose fatty acid esters, obtained by plotting $E_d(t)$ *versus* $\pi(t)$ at each time t: OF-C8m (A), OF-C8d (B), OF-C12m (C), OF-C12d (D), OF-C16m (E) and OF-C18m (F). Different symbols represent individual measurements on samples with varying bulk concentrations. The surface pressure at the CMC is indicated with a dashed line. Measurements were performed at 25 °C.

higher than π_{CMC}. For example, in the case of OF-C8d (Fig. 3B) the modulus decreases at $\pi > \pi_{CMC}$, while in the case of OF-C18m (Fig. 3F) the modulus increases at $\pi > \pi_{CMC}$. Possibly, the surface coverage may have reached a level where mesophase formation is occurring.

In addition to the oligofructose esters, the surface dilatational modulus of sucrose esters with chain lengths C12, C16 and C18 was studied. For all three sucrose esters, the modulus was determined at a fixed bulk concentration of 0.2% (w/v), higher than the CMC. For an interface stabilized by S-C12m, we have found a low surface dilatational modulus of 3.4 mN m^{-1} (Table 1). For sucrose esters with chain lengths C16 and C18 we found higher dilatational moduli of 15.0 mN m^{-1} and 29.4 mN m^{-1}, respectively. The higher modulus for the more

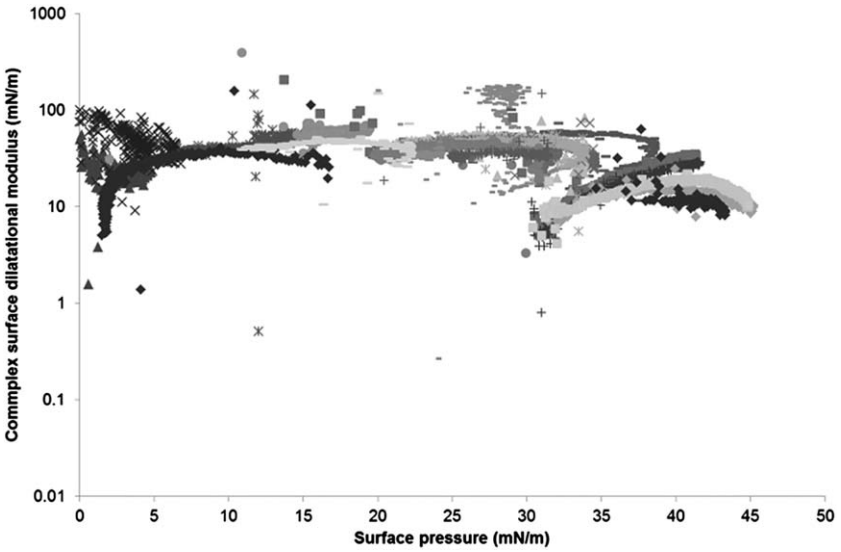

Fig. 4 Complex surface dilatational modulus as a function of surface pressure of air/water interfaces stabilized by OF-C16:1m, obtained by plotting $E_d(t)$ *versus* $\pi(t)$ at each time *t*. Different symbols represent individual measurements on samples with varying bulk concentrations. Measurements were performed at 25 °C.

hydrophobic sucrose esters may be explained using a similar reasoning as for the oligofructose esters: with increasing hydrophobicity the affinity for the interface increases, and the exchange with the subphase is slower.

In summary, the dependence of the surface dilatational modulus on the surface pressure of interfaces stabilized by oligofructose esters is quite difficult to interpret due to the high amount of variability in the data.

3.2 Traditional approach to surface rheology: dependence of the modulus on frequency

To gain more information about the rheological properties of the interfaces stabilized by different esters, frequency sweeps were performed after reaching equilibrium. Fig. 5 shows an illustrative result for OF-C12m.

The slope of a double logarithmic plot of complex surface dilatational modulus as a function of frequency was determined. These slopes are plotted as a function of the surface pressure in Fig. 6.

At surface pressures lower than π_{CMC}, for all esters the slope of the curve is low. A slope that approaches zero is an indication of a purely elastic interface. It shows that the migration of the esters from the bulk to the interface and *vice versa* upon compression and extension is very slow and that at this time scale no dissipative processes could be measured. This slow migration is the result of the relatively low concentration of the surfactant in the subphase.

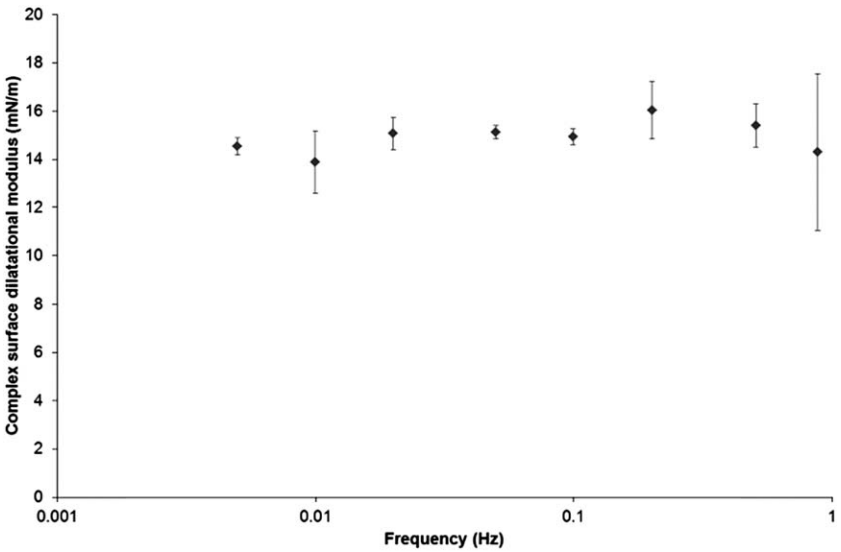

Fig. 5 Complex surface dilatational modulus of air/water interfaces stabilized by OF-C12m as a function of frequency determined at a bulk concentration of 0.02% (w/v). The figure shows the average and standard deviation of two measurements. Measurements were performed at 25 °C.

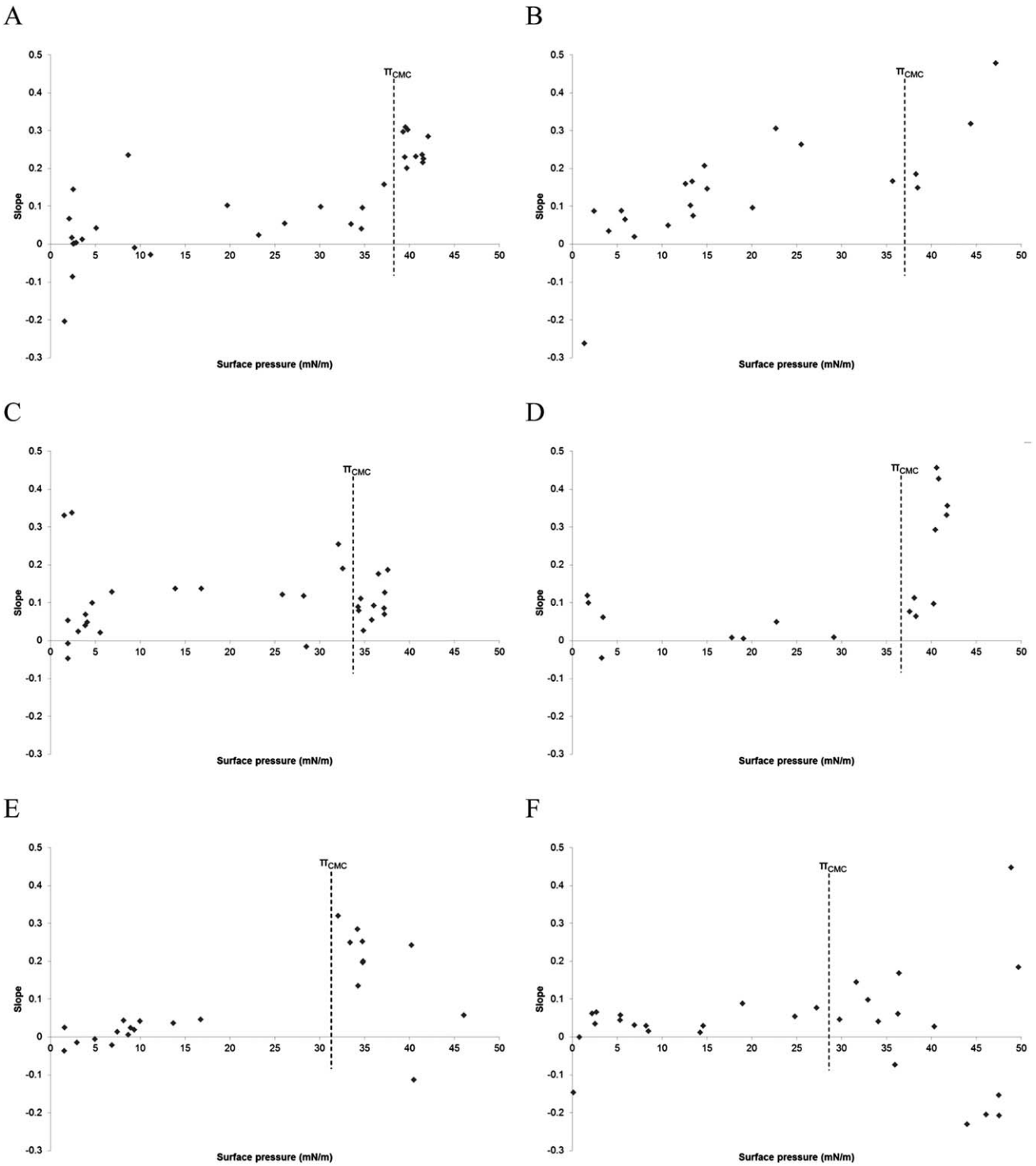

Fig. 6 Slope of a double logarithmic plot of complex surface dilatational modulus as a function of frequency obtained for air/water interfaces stabilized by oligofructose fatty acid esters. OF-C8m (A), OF-C8d (B), OF-C12m (C), OF-C12d (D), OF-C16m (E) and OF-C18m (F). The surface pressure at the CMC is indicated with a dashed line. Measurements were performed at 25 °C.

There is quite a bit of variation in the slope, especially at surface pressures higher than π_{CMC}. At similar surface pressures, different values in the slope are found for the different esters. Also in this case, the high degree of variability complicates the interpretation of the data. For OF-C16m (Fig. 6E), for example, at a surface pressure of 35 mN m^{-1} the slope varies between 0.12 and 0.3. In some cases, even negative values for the slopes were found. We will elaborate on these negative values in the next section. Despite these variations, for all mono-esters (Fig. 6A, C, E and F) the slopes remain relatively low at high surface pressures, and the rheological response appears not to be diffusion-controlled. This could be indicative

of the presence of interfacial mesophases, such as a soft glass phase formed by the oligofructose part, or a crystalline phase formed by the fatty acid chains. Such interfacial structures would be quite brittle, meaning that they are very sensitive to structure deformations, and could fracture or yield when the amplitude of deformation is too high. This could also explain the high variability in the slopes. Only in the case of OF-C8d (Fig. 6B) and OF-C12d (Fig. 6D) the slopes approach 0.5 at high surface pressures. These esters seem to behave like typical low molecular weight (LMW) surfactants, where the surface processes are diffusion-controlled, and adequately described by the Lucassen van den Tempel model.[9]

In a previous paper,[18] we have reported the interfacial area per molecule occupied by the oligofructose esters. We found that both mono-esters (67–94 Å^2) and di-esters (113–137 Å^2) occupy a significantly larger area than a single fatty acid chain (approximately 20 Å^2). The larger surface area per molecule is the result of the size of the oligofructose part of the molecule. Only when fatty acid chains are able to approach each other closely, will interactions between them lead to an interface with a high dilatational modulus and a low frequency dependence. Therefore, it is unlikely that the rheological properties that were found are the result of interactions between the fatty acid chains, for example crystallization. It is more likely that interactions between the oligofructose part are responsible for the rheological response, for example by the formation of a soft interfacial glass phase. The higher degree of polymerization of the oligofructose part compared to the sucrose part causes a shift in the glass transition, which may explain why the glass phase is formed for the oligofructose ester but not for the sucrose ester. Because di-esters occupy a slightly larger area than mono-esters, we hypothesize that two fatty acid tails might occupy slightly more interfacial area than the oligofructose part (Fig. 7). This could explain why, for di-esters, a slope of 0.5 is approached at high surface pressures: the oligofructose part cannot approach close enough to form a soft glass phase due to the presence of the two fatty acid chains.

The frequency dependence of OF-C16:1m (Fig. 8) was comparable to the frequency dependence of OF-C16m (Fig. 6E), with low slopes at low surface pressures and a high degree of variability at higher surface pressures caused by the high brittleness of the interfacial structure.

If the oligofructose part indeed forms a soft interfacial glass phase, the rheological properties of air/water interfaces stabilized by esters with a smaller hydrophilic group should be different. Therefore, we have studied the frequency dependence of the complex modulus of an air/water interface stabilized by sucrose esters. For S-C12m we found a slope of 0.26 (Table 1). For the other sucrose esters, we found slopes close to 0.5 (0.53 for S-C16 and 0.44 for S-C18), close to the frequency dependence predicted by the Lucassen van den Tempel model.[9] This would indicate that the surface processes are diffusion-controlled and that the higher modulus that is found for S-C16 and S-C18 compared to S-C12m is a result of slower exchange of molecules between bulk and interface. The slower exchange is caused by an increased hydrophobicity, which is caused by a longer fatty acid chain length and the presence of di-esters. This shows that the rheological response of sucrose esters is typical for LMW surfactants.

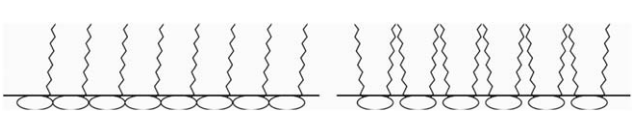

Fig. 7 Schematic representation of the proposed interfacial structure of oligofructose fatty acid esters. The oligofructose part is a mixture of oligomers with different degrees of polymerization between 2 and 8. Left: mono-esters, where the oligofructose part can approach closely and form a two-dimensional glass phase. Right: di-esters, where the incorporation of the second fatty acid chain prevents the close approach of the oligofructose part and glass phase formation.

3.3 Detailed study of the amplitude dependence of the modulus

In Sections 3.1 and 3.2, a traditional approach to surface rheology was followed. Some conclusions could be drawn based on the results that were obtained. However, the high degree of variability in the data that are presented in Fig. 3, 4, 6 and 8 complicates the interpretation of the data. We hypothesized that these variations are caused by the brittleness of the structures that are present at the interface. Therefore, in this section we will focus on the amplitude dependence of the modulus.

3.3.1 First-harmonic Fourier moduli. While amplitude sweeps are considered common practice in bulk rheology, in interfacial rheology they are far less commonly used. However, it is to be expected that any structure that is present on an interface (for example a two-dimensional network formed by a protein, or in our case a soft glass phase formed by the oligofructose part of the ester) will be affected when the deformation amplitude becomes too high. Especially for structures that are expected to be brittle, it is essential to know if the deformation amplitude that is applied is within the linear viscoelastic regime.

To find the dependence of the modulus on the deformation amplitude, an amplitude sweep was performed where, after reaching equilibrium, the amplitude was increased from the lowest amplitude that could be properly executed by the equipment (1.5%) to a very high value (30%). Fig. 9 shows an example of a typical curve of complex surface dilatational modulus *versus* amplitude obtained for air/water interfaces stabilized by OF-C18m at surface pressures higher than π_{CMC}. The results show that the surface dilatational modulus is strongly dependent on the applied amplitude. It continuously decreases as the amplitude increases. This may show that the interfacial structure is affected by the imposed deformation. Furthermore, it is obvious from these data that even the smallest amplitude that could be applied fell outside of the linear viscoelastic regime. The fact that the measurements were performed outside of the linear regime may explain the high degree of variability (as discussed in Section 3.1), and the negative values for the scaling exponent in the frequency dependence of the modulus (Section 3.2); during the frequency sweeps the structure was affected by the applied deformation. These results clearly indicate the importance of understanding

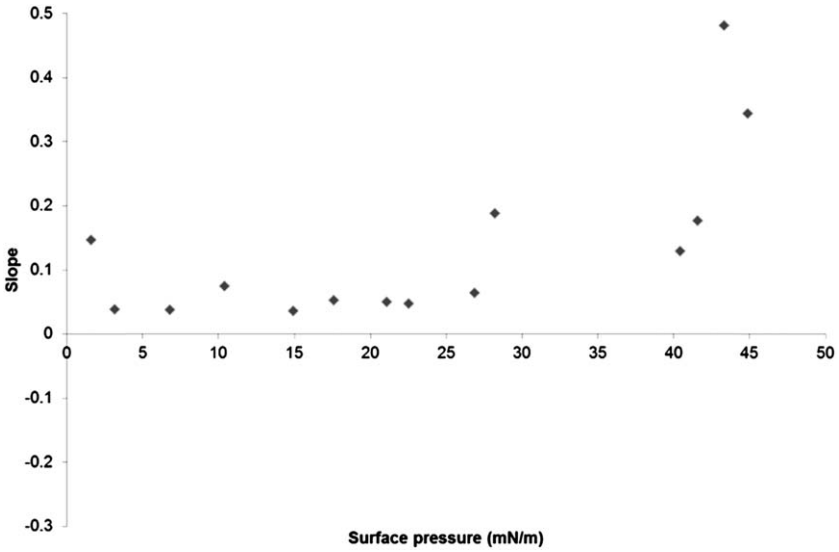

Fig. 8 Slope of a double logarithmic plot of complex surface dilatational modulus as a function of frequency obtained for air/water interfaces stabilized by OF-C16:1m. Measurements were performed at 25 °C.

Table 1 Complex surface dilatational modulus and the slope of a double logarithmic plot of surface dilatational modulus *versus* frequency determined for air/water interfaces stabilized by sucrose esters with chain lengths 12, 16 and 18 determined at a bulk concentration of 0.2% (w/v). Measurements were performed at 25 °C

Ester	Complex surface dilatational modulus (mN m^{-1})	Slope
S-C12m	3.4 ± 1.0	0.26 ± 0.042
S-C16	15.0 ± 1.3	0.53 ± 0.019
S-C18	29.4 ± 4.0	0.44 ± 0.014

the impact of the magnitude of deformations on the interfacial structure and are indicative of the presence of a brittle structure at the interface.

3.3.2 Lissajous plots. There are certain disadvantages in using the first-harmonic Fourier moduli that are the output of the equipment. As pointed out by Ewoldt *et al.*,[15] by using these first-harmonic Fourier moduli any nonlinearities that could be present in the raw signal are disregarded. Recently, the use of Lissajous plots of stress or surface pressure *versus* deformation has gained interest in interfacial rheology. Erni and Parker[19] have demonstrated how Lissajous plots can be used to analyze non-linearities in large amplitude surface shear rheology of Acacia gum. Rühs *et al.*[20,21] have demonstrated the usefulness of

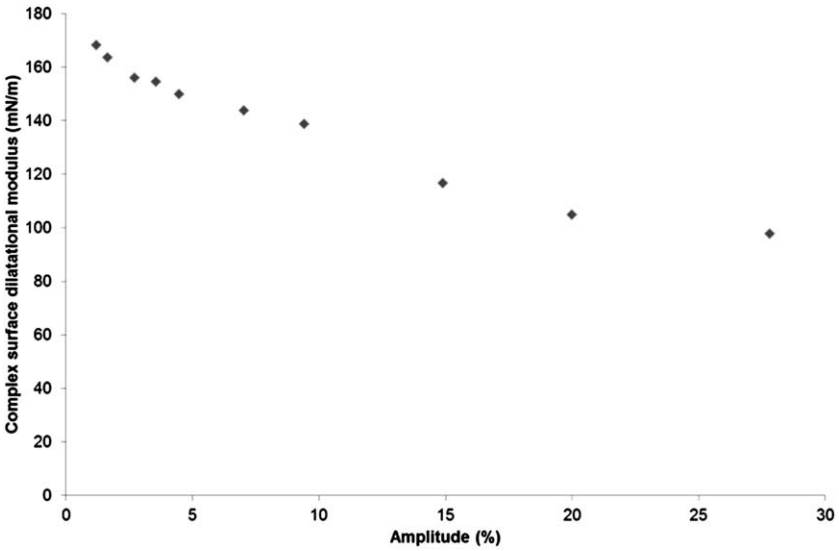

Fig. 9 Complex surface dilatational modulus as a function of amplitude for an air/water interface stabilized by OF-C18m at a bulk concentration of 0.05% (w/v). Measurements were performed at 25 °C.

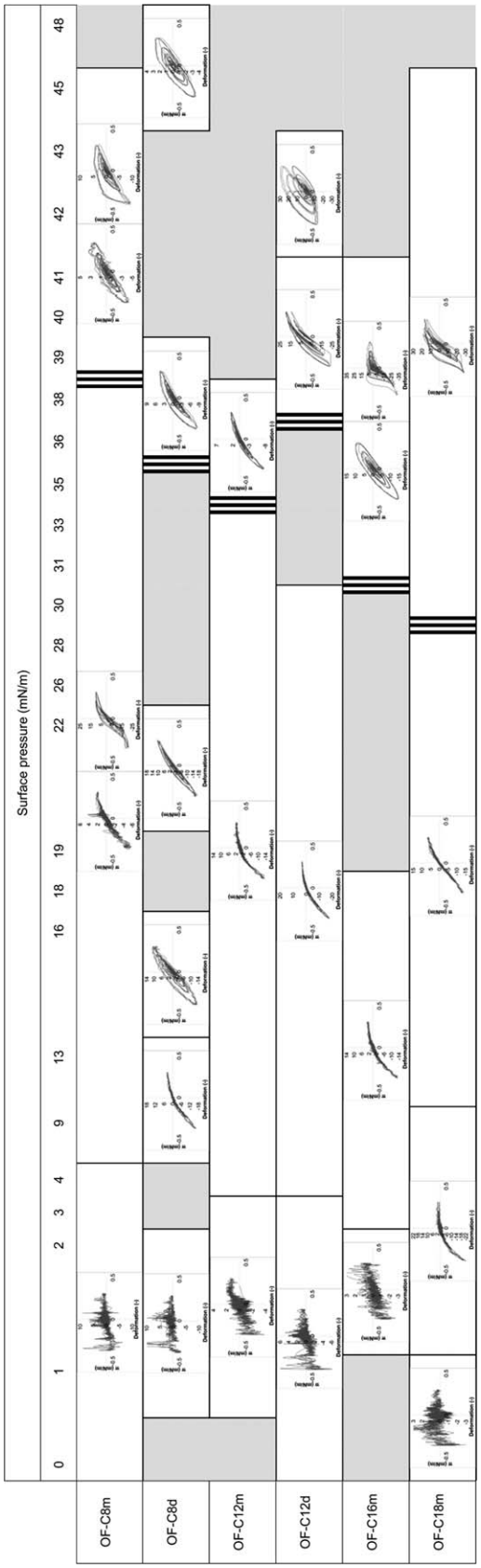

Fig. 10 Typical Lissajous plots at different surface pressure ranges obtained during amplitude sweeps of air/water interfaces stabilized by oligofructose fatty acid esters. The transition from $\pi < \pi_{CMC}$ to $\pi > \pi_{CMC}$ is clearly marked with a triple bold line. Measurements were performed at 25 °C.

Lissajous plots in analyzing interfacial rheology of β-lactoglobulin fibrils and monomers. In this paper the results of the amplitude sweeps are also presented as Lissajous plots (Fig. 10). The shape of the plots strongly depends on the surface pressure. Fig. 10 shows the Lissajous plots as a function of surface pressure for all oligofructose (saturated) mono-esters and di-esters. We have depicted the most common response over a certain range of surface pressures. In some cases, however, there were minor deviations.

For all esters, at extremely low surface pressures of 0–3 mN m^{-1}, the curves show only noise, which is caused by a too low surface concentration of esters.

In the range of surface pressures between 3 and π_{CMC} the response is, for all esters, predominantly elastic. These findings are consistent with the findings in Fig. 6, where a low frequency dependence of the modulus was found, indicating that the migration of the esters from the interface to the bulk and back again to the interface upon compression and extension was slow. Furthermore, in extension, the slope of the curves is decreasing with increasing amplitude, which points to strain softening. In contrast, in compression, the slope of the curves is increasing with increasing amplitude, which points to strain hardening. The degree of non-linearity becomes more pronounced with increasing deformation amplitude which shows that, even at low equilibrium surface concentrations, the surface may still become concentrated at high compressions.

At surface pressures higher than π_{CMC}, the degree of variability in the shape of the plots slightly increased. For OF-C8d and OF-C12d with increasing surface pressure the shape of the curves changes from mostly elastic, with strain hardening in compression and strain softening in extension, to more viscous without asymmetries. This is consistent with the frequency sweeps, where scaling exponents close to 0.5 were found at high surface pressures. For the oligofructose mono-esters, in most cases a response with strain hardening during compression and strain softening during extension was found. Combined with the low frequency dependence, this is consistent with the formation of a soft glass phase by the oligofructose part.

The shape of the Lissajous plot of OF-C16:1m (Fig. 11, obtained at high surface pressure) was similar to the one obtained for OF-C16m (Fig. 10) with strain hardening during compression and strain softening during extension. With increasing amplitude the response became more viscous. The shape of the curves of surface dilatational modulus *versus* surface pressure (Fig. 3E and 4) and of frequency dependence *versus* surface pressure (Fig. 6E and 8) were also similar. This shows that there were no major differences in the rheological response when the degree of saturation of the fatty acid chain was varied. This supports the earlier hypothesis that it is unlikely that interactions between the fatty acid chains are responsible for the rheological response. Instead, it supports the hypothesis that interactions between the oligofructose part are responsible.

The Lissajous plots that were obtained with sucrose esters (Fig. 12) were quite different than the ones obtained with oligofructose mono-esters. For all sucrose esters, the response was fairly viscous without any asymmetries. Combined with the exponent in the frequency dependence close to 0.5 it can be

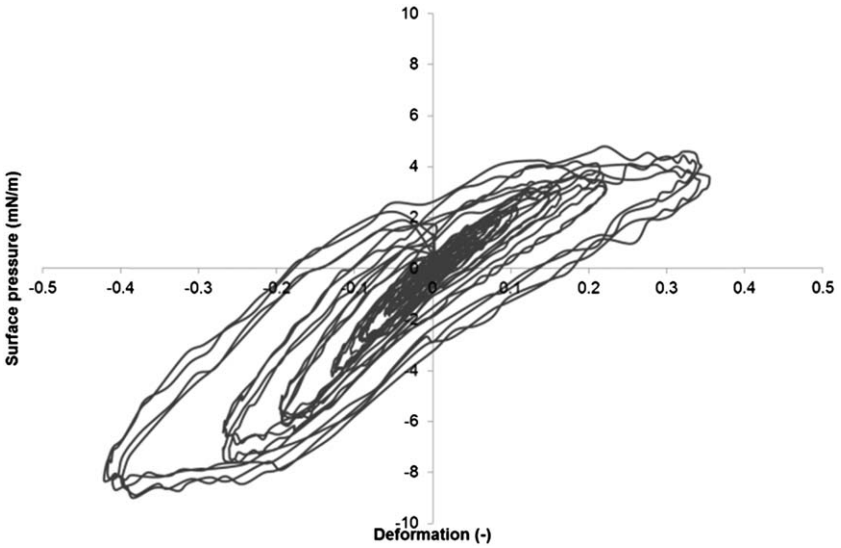

Fig. 11 Lissajous plot obtained during amplitude sweep of an air/water interface stabilized by OF-C16:1m. Measurements were performed at 25 °C.

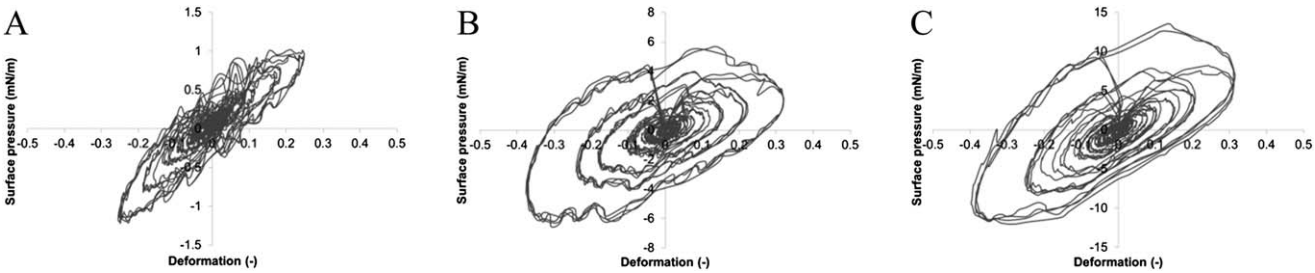

Fig. 12 Lissajous plots obtained during amplitude sweep of an air/water interface stabilized by sucrose esters. S-C12m (A), S-C16 (B) and S-C18 (C). Measurements were performed at 25 °C.

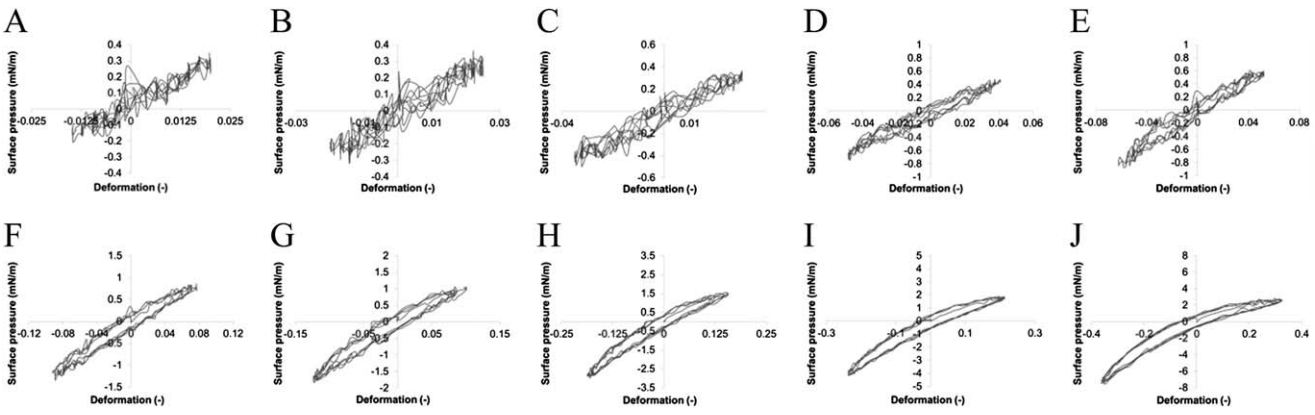

Fig. 13 Lissajous plots as a function of deformation amplitude for OF-C12m at a bulk concentration of 0.2% (w/v). Applied amplitude was 1.5% (A), 2% (B), 3% (C), 4% (D), 5% (E), 7.5% (F), 10% (G), 15% (H), 20% (I) and 30% (J). Measurements were performed at 25 °C.

concluded that there is no mesophase formation for sucrose esters and that they behave like typical LMW surfactants.

Next, some of the Lissajous plots in Fig. 10 were selected for further analysis. While for some esters, for example OF-C12m, the shape of the curve does not seem to depend on the deformation amplitude, for other esters, for example OF-C18m, clear deviations in the shape of the curves are observed when the deformation amplitude increases. Therefore, the dependence of the shape of the Lissajous plot on the deformation amplitude was examined for OF-C12m and OF-C18m in more detail.

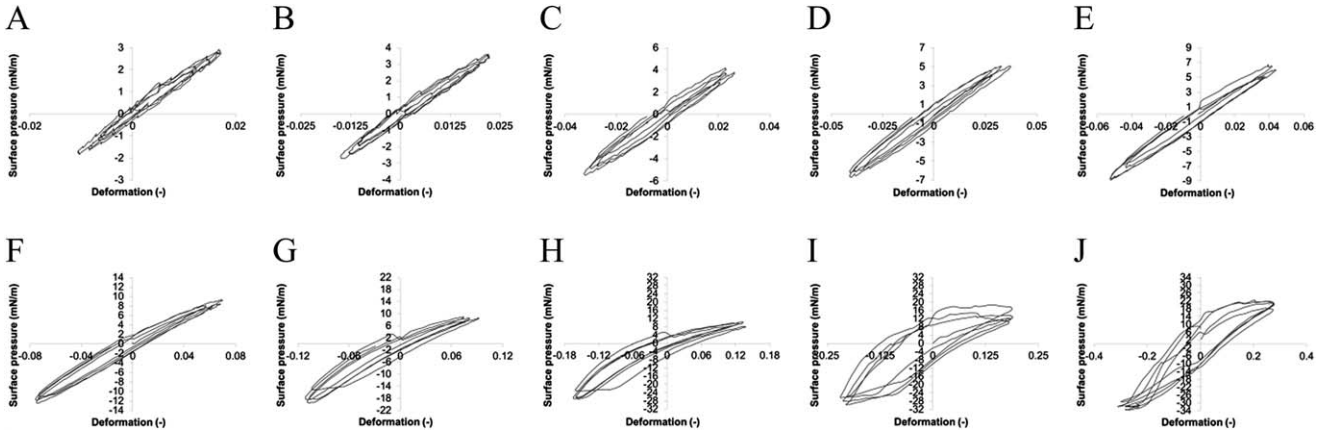

Fig. 14 Lissajous plots as a function of deformation amplitude for OF-C18m at a bulk concentration of 0.05% (w/v). Applied amplitude was 1.5% (A), 2% (B), 3% (C), 4% (D), 5% (E), 7.5% (F), 10% (G), 15% (H), 20% (I) and 30% (J). Measurements were performed at 25 °C.

For OF-C12m, at amplitudes up to 7.5% the Lissajous plots are characterized by a mostly elastic response, without pronounced asymmetries (Fig. 13A–F). At higher amplitudes the response becomes increasingly more asymmetric with strain hardening during compression and strain softening during extension (Fig. 13G–J).

Compared to OF-C12m (Fig. 13), for OF-C18m the shape of the Lissajous plots changes more when the deformation amplitude is increased (Fig. 14). These data represent the same dataset as presented in Fig. 9. At amplitudes up to 7.5% (Fig. 14A–F), the response is mostly elastic, without non-linearities. At 10 and 15% amplitude (Fig. 14G and H), the response is still mostly elastic, however here non-linearities appear, with strain hardening during compression and strain softening during extension. At 20 and 30% amplitude (Fig. 14I and J), the response becomes more viscous and is strain softening both in extension and compression.

To quantify the degree of non-linearity, we have determined S_{ext} and S_{com} for both components. For details of this procedure, the reader is referred to the Materials and methods section. A value close to 0 corresponds to a linear elastic response, a positive value for the S factor refers to intracycle strain hardening, whereas a negative S factor refers to intracycle strain softening.

Fig. 15A confirms the absence of non-linearities at amplitudes up to 4% for OF-C12m. Furthermore it shows that with increasing deformation amplitude the degree of non-linearity increases, both in compression and extension. For OF-C18m, Fig. 15B confirms the absence of any non-linearities, with S factors close to 0, in the rheological response up to an amplitude of 7.5%. Furthermore, it shows that the degree of strain softening upon extension becomes increasingly larger when the amplitude is increased from 10% to 30%. Finally, it does confirm that, up to 15% amplitude, the response is strain hardening upon compression and, above 20% amplitude, the response is strain softening upon compression. The strain softening in compression for OF-C18m at amplitudes above 20% is different from the response of OF-C12m where over the whole range of amplitudes strain hardening in compression is obtained. When examining Fig. 14I and J in detail it is obvious that the response in compression is initially strain hardening, and changes to strain softening with increasing degree of

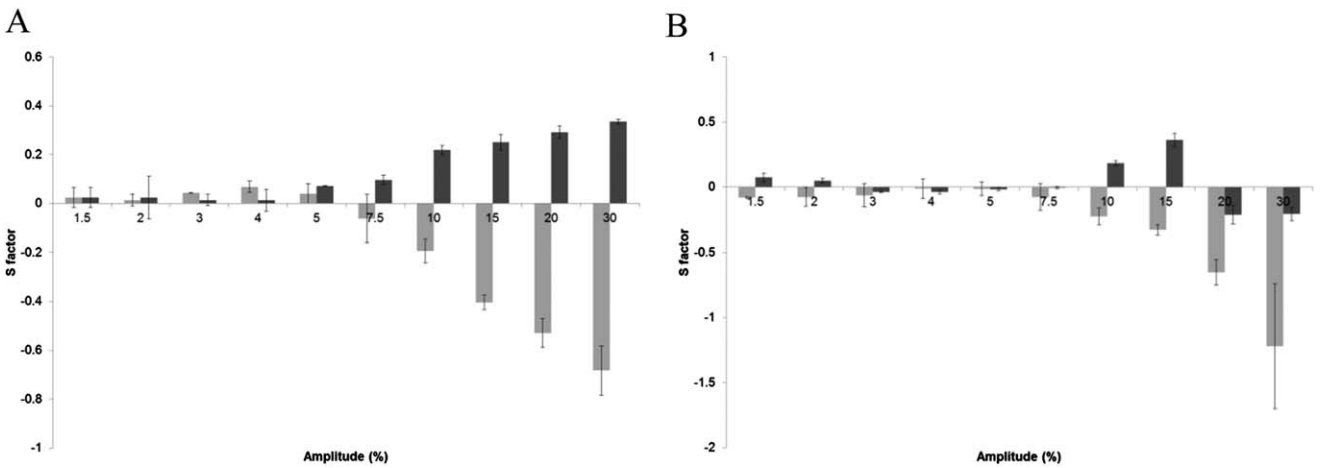

Fig. 15 S factor during extension (light grey) and during compression (dark grey), determined for amplitude sweeps of air/water interfaces stabilized by OF-C12m at a bulk concentration of 0.2% (w/v) (A) and by OF-C18m at a bulk concentration of 0.05% (w/v) (B). Measurements were performed at 25 °C.

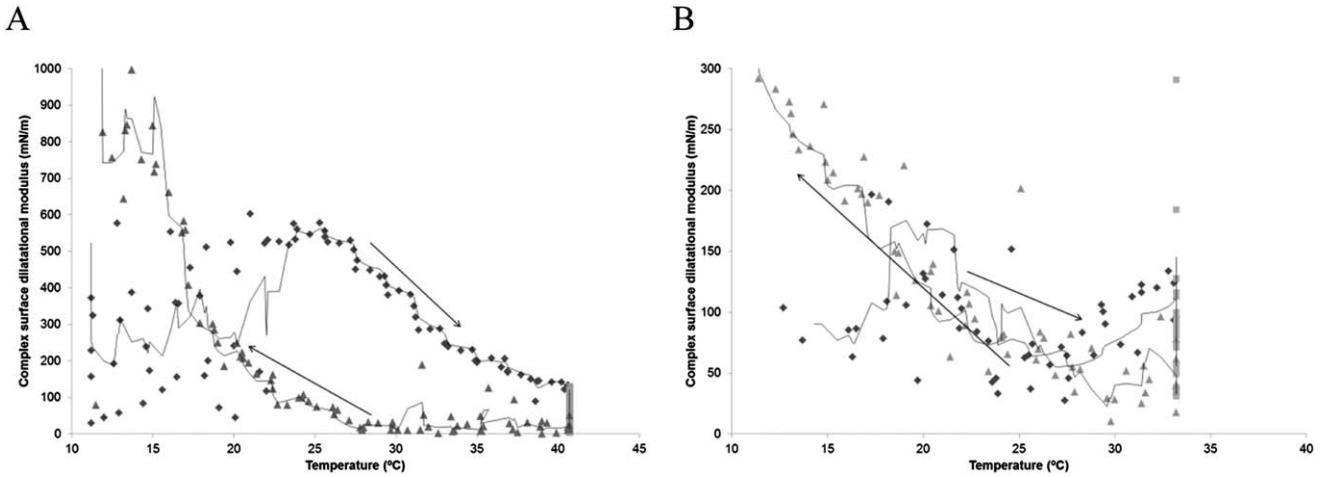

Fig. 16 Complex surface dilatational modulus of air/water interfaces stabilized by OF-C16m (A) and OF-C18m (B) as a function of temperature determined at a bulk concentration of 0.02% (w/v). The arrows indicate whether data points correspond to heating or cooling of the interface.

compression. This may be attributed to the occurrence of a rearrangement in the interfacial structure. A possible scenario is that with increasing deformation amplitude, cracks begin to form in the soft glass phase that eventually lead to the presence of individual islands of glass phase. These islands could start to slide on top of each other at very high deformations leading to strain softening. Furthermore, it is possible that the interfacial structure starts to buckle, and even expels part of the interfacial structure into the bulk in the form of a micelle. This scenario would also lead to strain softening. All these hypotheses need to be confirmed using appropriate techniques, such as Brewster Angle Microscopy, particle tracking observed by microscopy,[22] or grazing incidence X-ray diffraction.[23]

3.4 Dependence of the surface dilatational modulus on temperature

The results that have been described in Section 3.3 are in line with the hypothesis of the formation of a glass phase by the oligofructose part. Since the formation of a glass phase is a temperature-dependent process, the development of the modulus should be dependent on temperature as well. Therefore, temperature sweeps have been performed (Fig. 16) for OF-C16m and for OF-C18m.

The experiment was started with the establishment of an equilibrium at 10 °C. After equilibrium was established, the temperature was slowly increased to 42 °C in the case of OF-C16m (Fig. 16A) and 33 °C in the case of OF-C18m (Fig. 16B), and then slowly decreased again. During the warming up of the interface there is no clear dependence of the modulus on temperature; the initial modulus is also not extremely high. Since it is now clear that the interfacial structure depends on the magnitude of the imposed deformation it is likely that the interfacial structure development was hindered by deformation. Upon cooling a strong increase in surface dilatational modulus is visible as the temperature decreases. This is indicative of an interfacial structural transition, which is in support of the hypothesis that the eventually high dilatational modulus is a result of glass formation by the oligofructose part. Since non-ionic surfactants generally become more soluble in the bulk when the temperature is decreased and thus get a lower affinity for the interface, it is unlikely that the increase in dilatational modulus with decreasing temperature may be attributed to changes in the solubility of the ester.

4 Conclusion

In this article, we show how a standard surface rheological approach where the surface dilatational modulus is determined as a function of surface pressure and frequency does not always provide sufficient information about the interfacial structure. We show that it is especially important to understand the dependence of the surface dilatational modulus on deformation amplitude and temperature. We demonstrate that the use of Lissajous plots in interfacial rheology can be a powerful tool to increase the understanding of the link between surface rheological response and interfacial structure. Therefore, we propose that for a full rheological characterization of an interface the dependence of the surface dilatational modulus on surface pressure, frequency, amplitude and temperature should be determined and that Lissajous plots should be used to increase the understanding of interfacial microstructure. We have shown that interfaces stabilized by oligofructose esters have very different rheological properties compared to those stabilized by sucrose esters. While sucrose esters behave like typical LMW surfactants with low moduli, a scaling exponent in the frequency dependence close to 0.5, and fairly viscous Lissajous plots without asymmetries, oligofructose esters behave much differently. They form interfaces with relatively high moduli, low frequency dependence of the modulus and fairly elastic Lissajous plots with strain hardening during compression and strain softening during extension. We argue that the unusual rheological properties of interfaces stabilized by oligofructose fatty acid esters are most likely governed by the formation of a soft glass phase by the oligofructose part. This

hypothesis needs to be further investigated using appropriate structural characterization techniques.

Acknowledgements

This research forms part of the research program of the Dutch Polymer Institute DPI, project #687. The authors want to thank Carmen Boeriu for her contribution to the synthesis of the oligofructose fatty acid esters. Finally, we thank Acatris for supplying the RYOTO sucrose esters.

References

1 G. M. Campbell and E. Mougeot, *Trends Food Sci. Technol.*, 1999, **10**, 283–296.
2 S. A. Koehler, S. Hilgenfeldt and H. A. Stone, *Langmuir*, 2000, **16**, 6327–6341.
3 R. Miller, J. K. Ferri, A. Javadi, J. Krägel, N. Mucic and R. Wüstneck, *Colloid Polym. Sci.*, 2010, **288**, 937–950.
4 D. O. Grigoriev, S. Derkatch, J. Krägel and R. Miller, *Food Hydrocolloids*, 2007, **21**, 823–830.
5 L. Liggieri and R. Miller, *Curr. Opin. Colloid Interface Sci.*, 2010, **15**, 256–263.
6 M. A. Bos and T. Van Vliet, *Adv. Colloid Interface Sci.*, 2001, **91**, 437–471.
7 J. M. Rodríguez Patino, C. C. Sánchez and M. R. Rodríguez Niño, *Food Hydrocolloids*, 1999, **13**, 401–408.
8 J. M. Rodríguez Patino, C. C. Sánchez, M. R. Rodríguez Niño and M. C. Fernández, *Langmuir*, 2001, **17**, 4003–4013.
9 J. Lucassen and M. Van Den Tempel, *Chem. Eng. Sci.*, 1972, **27**, 1283–1291.
10 D. Langevin, *ChemPhysChem*, 2008, **9**, 510–522.
11 L. M. C. Sagis, *Rev. Mod. Phys.*, 2011, **83**, 1367–1403.
12 L. M. C. Sagis, C. G. Boeriu, G. E. Frissen, H. A. Schols and P. A. Wierenga, *Langmuir*, 2008, **24**, 359–361.
13 S. E. H. J. Van Kempen, K. Maas, H. A. Schols, E. Van der Linden and L. M. C. Sagis, *Food Hydrocolloids*, 2013, **32**, 162–171.
14 S. E. H. J. Van Kempen, C. G. Boeriu, H. A. Schols, P. De Waard, E. Van der Linden and L. M. C. Sagis, *Food Chem.*, 2013, **138**, 1884–1891.
15 R. H. Ewoldt, A. E. Hosoi and G. H. McKinley, *J. Rheol.*, 2008, **52**, 1427–1458.
16 G. Loglio, P. Pandolfini, R. Miller, A. Makievski, J. Krägel and F. Ravera, *Phys. Chem. Chem. Phys.*, 2004, **6**, 1375–1379.
17 E. Guzmán, L. Liggieri, E. Santini, M. Ferrari and F. Ravera, *J. Phys. Chem. C*, 2011, **115**, 21715–21722.
18 S. E. H. J. Van Kempen, H. A. Schols, E. Van der Linden and L. M. C. Sagis, 2013, submitted.
19 P. Erni and A. Parker, *Langmuir*, 2012, **28**, 7757–7767.
20 P. A. Rühs, C. Affolter, E. J. Windhab and P. Fischer, *J. Rheol.*, 2013, **57**, 1003–1022.
21 P. A. Rühs, N. Scheuble, E. J. Windhab and P. Fischer, *Eur. Phys. J.: Spec. Top.*, 2013, **222**, 47–60.
22 E. Van Der Linden, L. Sagis and P. Venema, *Curr. Opin. Colloid Interface Sci.*, 2003, **8**, 349–358.
23 V. M. Kaganer, H. Möhwald and P. Dutta, *Rev. Mod. Phys.*, 1999, **71**, 779–819.